

Quantum confinement of holes in $\text{Si}_{1-x}\text{Ge}_x/\text{Si}$ quantum wells studied by admittance spectroscopy

Fang Lu, Jiayu Jiang, and Henghui Sun

Fudan T. D. Lee Physics Laboratory, Fudan University, Shanghai, China

Dawei Gong, Xiangjiu Zhang, and Xun Wang

Surface Physics Laboratory, Fudan University, Shanghai, China

(Received 13 June 1994; revised manuscript received 11 October 1994)

A carrier thermal-emission model is presented to analyze the emission and capture of carriers in the admittance spectroscopy of $\text{Si}/\text{Si}_{1-x}\text{Ge}_x/\text{Si}$ quantum wells. The experimental activation energy is related to the band offset at the interface of the SiGe well and the Si barrier as well as the confined hole-energy level in the well. The measured band offset for a single quantum well with Ge content of 0.33 is much closer to the theoretical prediction than that derived from the equivalent circuit model. The quantum size effects for both single-quantum-well and multiple-quantum-well samples are clearly revealed by the peak shifts of the conductance spectra. The emissions of holes from the confined heavy-hole subband and the light-hole subband in multiple-quantum-well samples with small well widths appear as a distinct doublet in the conductance spectra.

I. INTRODUCTION

The admittance spectroscopy was developed in the 1970s to study deep-level defects in bulk semiconductors.¹ Similar to deep-level transient spectroscopy (DLTS), the principle of the admittance spectroscopy is also based on the thermal emission and capture of carriers from deep-level defects. In the 1980s, Lang *et al.*² employed this method to determine the band offset in semiconductor quantum wells. The measurement technique is identical to the conventional admittance spectroscopy, but the analysis is somewhat different. To analyze the admittance spectra of quantum wells, Lang *et al.* established the relationship between the activation energy of carriers and the experimental parameters (measuring frequency and peak temperature) based on an equivalent circuit model, where the activation energy is the energy difference between the Fermi level and the top of the well. The band offset can be derived from the activation energy determined by the admittance measurement. Successful applications to both the lattice-matched and lattice-mismatched systems like $\text{Ga}_{1-x}\text{In}_x\text{As}/\text{InP}$, $\text{Al}_x\text{Ga}_{1-x}\text{As}/\text{GaAs}$, and $\text{Si}_{1-x}\text{Ge}_x/\text{Ge}$ have been achieved.²⁻⁴ As for the experimental methods, a single-frequency admittance-spectroscopy technique has been developed to simplify the measurement procedures.⁵ Since the admittance spectrum of a quantum well is mainly contributed to the emission and capture of carriers confined in the subbands of the quantum well across the potential barrier, it is thus possible to employ this method to study the carrier confinement effect in quantum wells. However, in order to obtain some quantitative information concerning the subband structures, we found that the equivalent circuit model is not sufficient. In this work, another data processing method, i.e., the carrier thermal-emission model, based on analyzing the exchange of holes between the subbands and the valence band under small ac voltage signal, is proposed. The emission

and capture of confined holes in the subbands of $\text{Si}_{1-x}\text{Ge}_x\text{Si}$ single and multiple quantum wells have been revealed by the admittance-spectroscopy measurements. Double-peak conductance spectra observed in multiple-quantum-well samples with small well widths are attributed to the hole emission and capture from ground-state heavy-hole and light-hole subbands based on the carrier thermal-emission model.

II. PRINCIPLE OF MEASUREMENT

If a quantum well of holes is located adjacent to a Schottky contact on the top of the cap layer, the potentials and thus the valence bands of the quantum well and Schottky barrier under different bias voltages could be obtained by solving the Poisson equation. The results are shown in Fig. 1, where the distance from the quantum well to the Schottky contact is 300 nm and the doping concentrations in all regions are $2 \times 10^{16} \text{ cm}^{-3}$. The measurements of admittance spectra are carried out at zero bias. Under the small ac signal condition, the periodic variation of the valence band occurs basically at the left side of the well ($x=0$), as shown in Fig. 1. The interchange of holes between the subband in the quantum well and the valence band of the Si barrier leads to a change of hole concentration in the quantum well and, thus, generates the ac conductance and capacitance of the sample. Since the periodic emission and capture of holes occur near the thermal equilibrium, according to the detailed balance principle, the emission and the capture rate are the same.⁶ The expressions of ac conductance G and capacitance C are usually derived from the emission process.

If an ac signal $dV = dV_0 \exp(j\omega t)$ is applied to the sample, where ω is the angular frequency of the signal and t is the time, the current in the circuit is given by

$$i(t) = -\frac{dQ}{dt} = e_p Q(t), \quad (1)$$

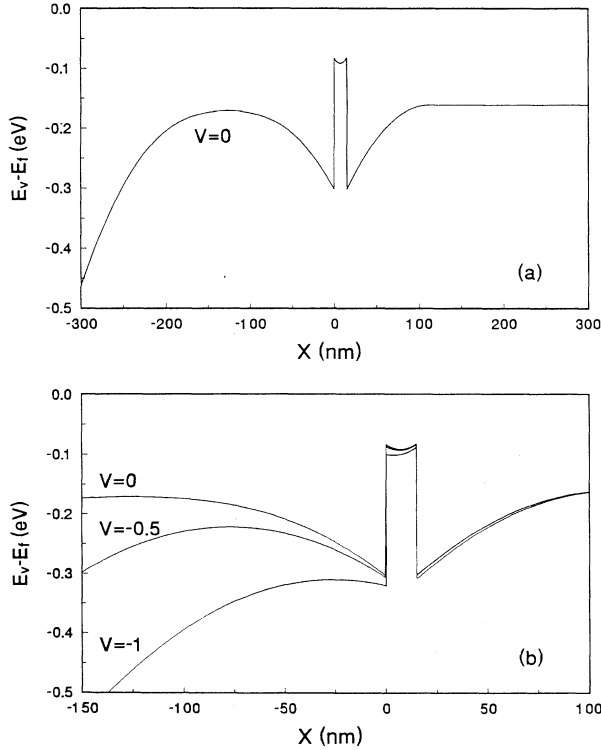


FIG. 1. Variation of valence band of a single quantum well at (a) zero bias and (b) under different voltages.

with

$$Q(t) = dQ(t) - \int_0^t i dt, \quad (2)$$

where e_p is the emission rate of holes in the well and $Q(t)$ is the charge in the well. Under the small signal condition, the variation of charges in the well could be approximately expressed as

$$dQ(t) = \beta dV, \quad (3)$$

where β is a parameter correlated with the hole concentrations in the well. By combining Eqs. (1)–(3), one obtains

$$i(t) = e_p \left[\beta dV - \int_0^t i dt \right]. \quad (4)$$

The mathematics of solving Eq. (4) and deriving the expressions of G and C are similar to that in Ref. 7. The results are

$$G = \frac{e_p \omega^2}{e_p^2 + \omega^2} \beta, \quad (5)$$

$$C = \frac{e_p^2}{e_p^2 + \omega^2} \beta + C_0, \quad (6)$$

where C_0 is the capacitance at low temperature where the carriers are almost fully frozen out.

For multiple-quantum-well samples, the solution of the Poisson equation shows that the variation of energy band with applied voltage occurs basically between the

Schottky contact and the first quantum well adjacent to it. The ac admittance of the sample is mostly contributed by the emission and capture of holes in the first quantum well. The above model holds also for multiple-quantum-well samples.

The emission rate of holes in a quantum well has been given by Debbar, Biswas, and Bhattacharya,⁶

$$e_p = \alpha T^{1/2} E_a^{3/2} \exp \left[-\frac{E_a}{kT} \right], \quad (7)$$

where α is a temperature independent constant and E_a is the activation energy, which is the energy difference between the subband and the top of the well, i.e.,

$$E_a = \Delta E_v - E_1, \quad (8)$$

where ΔE_v is the valence-band offset and E_1 is the energy level of the first subband with respect to the energy of the well bottom.

The temperature dependences of conductance and capacitance arise basically from e_p . At low temperatures, the carriers in the well are mostly frozen out. Therefore, $e_p \rightarrow 0$, and $G_L \rightarrow 0$, $C_L \rightarrow C_0$. At high temperatures, $e_p \gg \omega$ and $G_H \rightarrow 0$, $C_H = \beta + C_0$. The maximum of G occurs at $e_p = \omega$, and could be simply expressed as

$$G_{\max} = \frac{1}{2} \beta \omega. \quad (9)$$

Therefore, when the temperature scans from low to high, there is a peak in the conductance spectrum and a steep rise in the capacitance spectrum. From Eqs. (5)–(7), the temperature at conductance peak (T_m) is related to the measuring frequency ω by the following expression:

$$\omega = e_p(T_m) = \alpha (T_m)^{1/2} (E_a)^{3/2} \exp \left[-\frac{E_a}{kT_m} \right]. \quad (10)$$

By measuring the conductance spectra at different frequencies and plotting an Arrhenius curve $\ln(\omega/T_m^{1/2}) \sim 1/T_m$, the activation energy E_a and constant α could be obtained.

Once the parameters are determined, we can simulate the admittance spectra and compare them with the raw experimental data. From Eqs. (5), (6), and (9), we have

$$\frac{G_{\max}}{\omega} = \frac{1}{2} \beta = \frac{1}{2} \Delta C, \quad (11)$$

where

TABLE I. Structural parameters of the samples.

Sample	Ge content x	Well width (nm)	Barrier width (nm)	No. of periods
S1	0.33	15		1
S2	0.33	3.5		1
M1	0.33	3.5	25	5
M2	0.33	5	25	5
M3	0.33	15	30	10

$$\Delta C = C_H - C_L \quad (12)$$

Using Eq. (11), β could be determined by experimental values of G_{\max} . Substituting Ea , α , β , and C_0 into Eqs. (5)–(7), the G - T and C - T curves could be reconstructed. The agreement between the simulated admittance spectra and the experimental curves might be used as a test of the accuracy of the data-analysis method.

The expression of activation energy Ea above is somewhat different from that in the equivalent circuit model, where the activation energy is closely related to the Fermi level. While in our carrier-emission model, the conductance is based on the carrier emission and capture from the subband in a quantum well; the activation energy is the energy difference between the subband and the top of the well. So, it is feasible to investigate quantum confined states in quantum wells by using admittance spectroscopy. On the other hand, if the subband energy E_1 is known by theoretical calculation, the admittance-spectroscopy measurement could be used to determine the band offset.

III. EXPERIMENT

The samples were grown by molecular-beam epitaxy (MBE). The substrates used were p -type single-crystal Si(100) wafers with the resistivity of $0.05 \Omega \text{ cm}$. After epitaxially growing the Si buffer layer with the thickness of 200–300 nm, the $\text{Si}_{1-x}\text{Ge}_x/\text{Si}$ single quantum wells or multiple quantum wells were grown at the substrate temperature of 500°C . The structure parameters of the samples are shown in Table I. The $\text{Si}_{1-x}\text{Ge}_x$ alloys layers in the structures were formed by coevaporating the Si and Ge sources by two electron-beam evaporators. The Ge composition x and the layer thickness were monitored *in situ* by two quartz thickness monitors in the MBE system. All the layer thicknesses in Table I are controlled well below the critical thicknesses of pseudomorphic growth,⁸ so the quantum wells are fully strained. At the final state of epitaxy, a Si cap layer with the thickness of 300–400 nm was deposited on top of the quantum well. The wafers were then moved out from the vacuum to make the testing structures. An ohmic contact was made on the back side by evaporating Al and alloying in nitrogen at 500°C . On the front side, a Schottky contact was

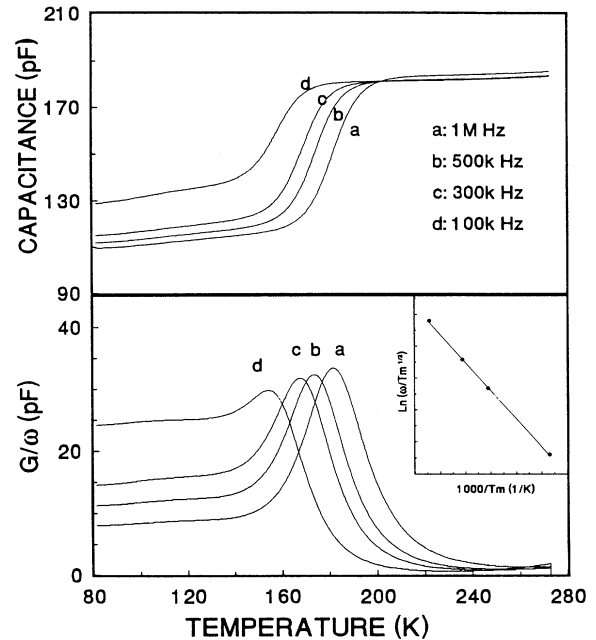


FIG. 2. Measured capacitance and conductance spectra at different frequencies

made by evaporating an Al dot with the diameter of 1 mm without alloying.

The admittance spectra were measured in the temperature range of 77–300 K at frequencies of 1 MHz, 500 KHz, 300 KHz, and 100 KHz by using a Hewlett-Packard 4275A LCR meter. The temperature of the sample was measured by a thermocouple with a FLUKE 8840A digital multimeter as the voltage indicator. Both meters were controlled by a computer through the IEEE-488 interfaces.

IV. RESULTS AND DISCUSSION

A. Single-quantum-well samples

Figure 2 shows the capacitance and conductance of sample S1 varying with temperature under different test-

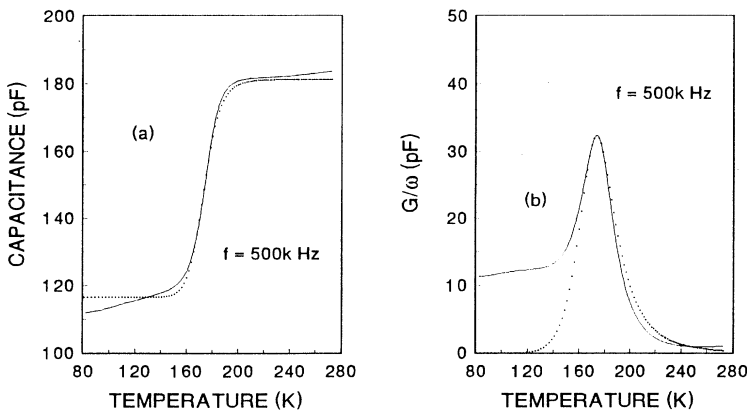


FIG. 3. Reconstruction of C - T (a) and G - T (b) curves by computer simulation (— experiment, - - - calculation).

ing frequencies at zero bias. With increasing frequency, the emission of carriers in the well requires higher temperatures to reach sufficient emission probability $e_p(T_m)$; the peak in conductance spectrum thus shifts toward higher temperatures. From the measured peak temperatures T_m at different frequencies, a $\ln(\omega/T_m^{1/2}) \sim 1/T_m$ plot could be drawn, as shown in the inset of Fig. 2. The activation energy of sample *S1* is determined to be $Ea = 0.20$ eV with the coefficient $\alpha = 1.585 \times 10^{12} K^{-1} eV^{-3/2} s^{-1}$ in Eq. (10). The correlation coefficient $\gamma = 0.9999$, verifies the linear relocation.

The reconstruction of G - T and C - T curves at $f = 500$ kHz have been done by using Eqs. (5)–(7) with the values of Ea , α above, and $G_{\max}/\omega = 32.3$ pF from Fig. 2. The results are shown in Fig. 3, where the dotted curves are reconstructed spectra and the solid curves are the experimental data. The deviation between the simulated and the experimental capacitance curves at the low-temperature side is basically due to the slight variation of C_0 with the temperature, which is ignored in the theoretical simulation. The origin of the large deviation between the simulated and experimental conductance curves at low temperatures is not very clear. One possibility is the contribution by the interfacial defects located near the boundaries of the quantum well. The emission and capture of carriers by the interfacial defects give rise to an additional conductance, which play the role only at low temperature when the carriers in the well are frozen out and thus could not follow the variation of the applied voltage. The emission and capture of holes by interfacial defects are frequency dependent. They could only partially respond to the ac voltage at high frequencies. Nevertheless, the major feature of interest is around the conductance peak and the steep rise of capacitance. The good agreement of this feature in experimental and theoretical simulation illustrates that the description of the admittance spectra of a quantum well by the carrier-emission model is acceptable.

Figure 4 shows the conductance spectrum of sample *S2* with respect to that of sample *S1* at the testing frequency of 1 MHz. The two samples possess the same Ge composition and thus the same well depth but different

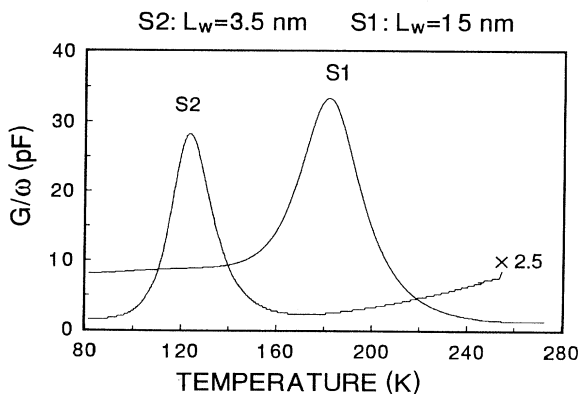


FIG. 4. Conductance spectra of two single-quantum-well samples.

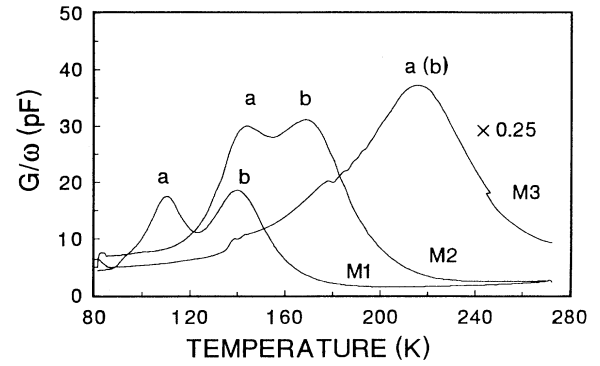


FIG. 5. Conductance spectra of three multiple-quantum-well samples.

well widths. The activation energy of sample *S2* is derived to be 0.17 eV, smaller than that of sample *S1*. Assuming a square-well model, the energy of the heavy-hole ground subband E_1 is 0.003 eV for sample *S1* and 0.03 eV for sample *S2*. The difference is 0.03 eV, which is the same as the difference in Ea . The band offset is 0.20 eV for both samples as expected. Therefore, the difference in activation energies is attributed to the shift of the ground subband with respect to the different well widths. The fact that the peak shifts toward lower temperature for a sample with a narrower well agrees qualitatively with the carrier-emission model.

The theoretically predicted band offset for a $Si_{0.67}Ge_{0.33}/Si$ heterointerface is 0.24 eV,⁸ a little larger than our result. The deviation may be caused by two reasons. First, the well shape is not exactly a square one due to the Ge segregation during the epitaxial growth. Second, in uniformly doped quantum-well structures, the transfer of carriers from barrier to well leads to the carrier accumulation in the well region and carrier depletion in the barrier region. The well shape influenced by the band bending is no longer squarelike, as shown in Fig. 1. The carrier emission could take place through thermally assisted tunneling with an apparent activation energy smaller than that of a square well. This also reduces the measured value of the band offset.

As a comparison, we also do the data treatments by using the equivalent circuit model. The Fermi level E_F with respect to the valence-band edge of $Si_{1-x}Ge_x$ at the interface is calculated by solving the Poisson equation. It is found that E_F lies within the band gap.⁵ Therefore, the band offset ΔE_v must be smaller than the activation energy and appears as 0.16 eV for samples *S1*. The deviation of ΔE_v from that of the theoretical prediction is more serious and harder to explain.

TABLE II. Activation energies of multiple-quantum-well samples (in eV).

Sample	<i>M1</i>	<i>M2</i>	<i>M3</i>
Activation energy (peak <i>a</i>)	0.12	0.15	0.21
Activation energy (peak <i>b</i>)	0.18	0.20	

TABLE III. Subbands in multiple-quantum-well samples (in eV).

Sample	Well width (nm)	Heavy-hole energy level	Light-hole energy level	Subband (HH1) emission energy	Subband (LH1) emission energy
<i>M1</i>	3.5	0.039	0.090	0.18	0.13
<i>M2</i>	5	0.023	0.058	0.20	0.16
<i>M3</i>	15	0.003	0.010	0.22	0.21

B. Multiple-quantum-well samples

Figure 5 shows the conductance spectra for three multiple-quantum-well samples with the same Ge composition but different well widths. Again, the quantum size effect, i.e., the peak shifts toward lower temperatures for narrower well widths, could be seen. The most interesting feature here is the double-peak structures of samples *M1* and *M2*. The spectrum of sample *M3* is a broad peak, which may be composed of two unresolved peaks. The activation energies of these peaks are listed in Table II. The high-temperature component (peak *b*) in doublet corresponds to the carrier emission from the heavy-hole ground subband in the well. The activation energies are comparable with but a little larger than those obtained for single-quantum-well samples. The low-temperature component (peak *a*) has not been reported in previous literature. It could not be explained by the equivalent circuit model, where only one conductance peak can occur corresponding to a single resonant frequency. Also it could not be originated from some deep-level defects as verified by the DLTS measurement. By calculating the hole subband structures of the multiple quantum wells within the framework of the Kronig-Penney model, we

obtain the energies of heavy-hole ground states (HH1) and light-hole ground states (LH1) with respect to the well bottom as shown in Table III. It could be seen that the emission energies from HH1 and LH1 agree well with the corresponding activation energies listed in Table II. Thus, it is not unreasonable to assign the double-peak conductance spectra to the carrier emission from the two hole subbands in the quantum wells.

V. CONCLUSIONS

We have demonstrated the successful use of the admittance spectroscopy to study the carrier confinement effect in $\text{Si}_{1-x}\text{Ge}_x/\text{Si}$ quantum wells. Not only the carrier emission and capture processes from the heavy-hole ground state but also the processes from the light-hole ground state are revealed in the admittance spectra of multiple-quantum-well samples.

ACKNOWLEDGMENT

This work was supported by the key project of the State Commission of Science and Technology.

¹D. L. Losse, J. Appl. Phys. **46**, 2204 (1975).

²D. V. Lang, M. B. Panish, F. Capasso, J. Allam, R. A. Hamm, A. M. Sergent, and W. T. T. Sang, Appl. Phys. Lett. **50**, 736 (1987); J. Vac. Sci. Technol. B **5**, 1215 (1987).

³X. Letartre, D. Stievenard, M. Lannoo, and D. Lippens, J. Appl. Phys. **68**, 116 (1990).

⁴K. Nauka, T. I. Kamins, J. E. Turner, C. A. King, J. L. Hoyt, and J. F. Gibbons, Appl. Phys. Lett. **60**, 195 (1992).

⁵F. Lu, J. Jiang, H. Sun, D. Gong, and Xun Wang, J. Appl. Phys. **75**, 2957 (1994).

⁶N. Debbar, D. Biswas, and P. Bhattacharya, Phys. Rev. B **40**, 1058 (1989).

⁷G. Vincent, D. Bois, and P. Pinard, J. Appl. Phys. **46**, 5173 (1975).

⁸Chris G. Van de Walle, Phys. Rev. B **34**, 5621 (1986).